Robust Reading Approach for Moving Chipless RFID Tags by Using ISAR Processing

Filippo Costa, *Member, IEEE*, Michele Borgese, Antonio Gentile, Luca Buoncristiani, Simone Genovesi, *Member, IEEE*, Francesco Alessio Dicandia, Davide Bianchi, *Member, IEEE*, Agostino Monorchio, *Fellow, IEEE*, Giuliano Manara, *Fellow, IEEE*

***Abstract*— A robust technique for reading moving chipless tags exploiting the Inverse Synthetic Aperture Radar (ISAR) data processing is presented. The procedure takes advantage from the known tag movement to improve the tag detection capability by integrating several received signals. The implicit advantage of the proposed detection scheme is that the background measurement, collected in the absence of the tag, can be easily performed before the tag passes in front of the reader antenna. The reading procedure allows for a significant increase of the reading distance and, more importantly, it greatly improves the detection probability in complex scenarios where the tag is attached on arbitrary and highly scattering objects. A simplified model is used to demonstrate the capabilities of the presented procedure in detecting tags even in the presence of high clutter. Detection of tags with Signal Noise Ratio (SNR) as low as −10 dB is experimentally demonstrated.**

***Index Terms*— Chipless RFID; Frequency Selective Surfaces (FSS), Inverse Synthetic Aperture Radar (ISAR).**

I. Introduction

CONVENTIONAL RFIDs are radio frequency labels comprising an antenna and an ASIC (Application Specific Integrated Circuit). The integration of the chip represents the major cost in the production of the RF labels. To drastically reduce the fabrication costs and allow these RF labels to work in extreme environments, a new paradigm has been explored in the last years: the chipless RFID. Chipless solutions can be implemented in different configurations but a fundamental distinction among chipless RFID tags can be made based on the codification method. One popular approach consists of storing information in the time domain (TD) response of the tag while another widespread paradigm is based on frequency domain (FD) codification [1]–[6]. Chipless RFID technology has also evolved towards sensing applications [7]–[10] as it is possible to translate environmental variations into a perturbation of the radio frequency response.

Manuscript received August 21, 2017. This work was supported by the H2020 Grant Agreement 645771– EMERGENT. F. Costa, M. Borgese, A. Gentile, L. Buoncristiani, S. Genovesi, F. A. Dicandia, D. Bianchi, A. Monorchio and G. Manara are with Department of Information Engineering, University of Pisa, 56122 - Pisa, Italy. L. Buoncristiani is now with U-blox. E-mail: filippo.costa@iet.unipi.it, michele.borgese@for.unipi.it.

Despite the lower fabrication cost, some drawbacks may prevent the adoption of chipless RFIDs in real world applications. One of the drawbacks is the limited read range. In fact, due to the large frequency range used for probing the tag, the reader transmitted power should be compliant with the regulations of ultra-wideband communications (UWB) [11]. The distance between the reader antenna and the tag cannot realistically exceed 50 cm.

The second and more critical issue of chipless RFID technology is the calibration procedure needed to remove undesired contributions of interference, such as the multipath deriving from objects in proximity to the tag and the antenna mismatch. Some approaches aimed at reading chipless tags with a single acquisition have been recently proposed in the literature [12], [13]. They exploit Fast Fourier Transform (FFT) of the received signal, temporal filtering and polarization properties of the tags. However, even if these procedures greatly contribute to improve the reading process, they provide good results only if there are no highly scattering object located in the vicinity of the tag. A more robust approach relies on the classical calibration procedure based on a preliminary acquisition of the background in absence of the tag [5], [6]. However, this approach requires at least two measurements for the detection of the tag. This kind of normalization is not feasible in real scenarios, except when it is possible to store the background response in advance. An interesting scenario, where the background subtraction is feasible, is the conveyor belt in which the tag moves with respect to a fixed reader antenna. Since the latter scenario is actually one of the most common in real applications of RFID, it deserves more attention than it has received to date. Some advantages of the conveyor belt scenario have been already exploited for conventional time modulated UHF-RFID [14]. However, the moving scenario has never been analyzed for chipless RFID. While the reading of UHF-RFIDs is a standardized practice and several readers are available in the market, the reading of chipless RFID is a very challenging problem [12], [13].

The purpose of this paper is to study the applicability of a single step measurement procedure to the moving scenario. Indeed, the fact that the tags move with respect to a fixed antenna gives an intrinsic advantage since the calibration can be easily performed by storing in advance the background response in absence of the tag in front of the antenna. In addition, as tags move along a conveyor belt, it is possible to perform several acquisitions of the same tag at different

angles. Consequently, an ISAR-based processing technique is proposed to drastically improve the reliability of the chipless tags reading process.

The paper is organized as follows. The analyzed scenario and the proposed reading approach is described in Section II. Section III is dedicated to the description of a simple analytical model of the analyzed problem which gives an immediate perception of the improvement of the tag detection in terms of Bit Error Rate (BER) provided by the proposed reading method. The results of an extensive measurement campaign of the chipless tag located in low and high scattering environments is reported in Sections IV, V and VI. Concluding remarks are drawn in Section VII.

II. Moving Tag Scenario

One of the most important limitations of chipless technology is the calibration procedure that is based on two independent measurements performed on the same scenario (tag and background and eventually reflective ground plane) [5], [6].

To avoid this unpractical calibration procedure, a realistic and typical scenario for RFID, where the background acquisition is possible, is investigated. We suppose that the tag is able to move along a linear trajectory with constant velocity, as in the case of conveyor belts in airport handling systems, parcel distribution centers or highly automated assembly lines. As depicted in Fig. 1, in a conveyor belt scenario, the tag may not be always located into the main beam of the reader antenna. Therefore, it is possible to perform a continuous acquisition of the scenario until the level of the measured signal increases relevantly. This corresponds to the appearance of the tag within the main beam of the reader antenna.

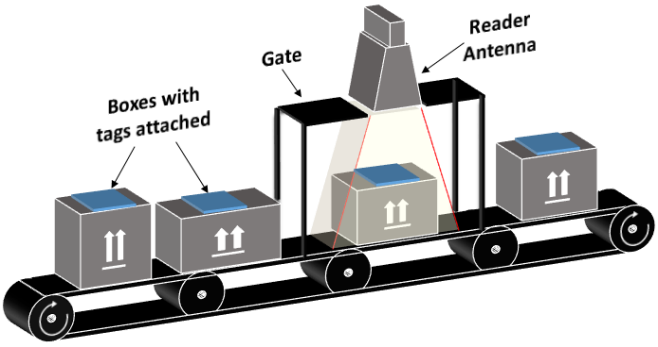

Fig. 1. Analyzed conveyor belt scenario for chipless RFIDs.

The *background-measurement*, which is stored before the arrival of the tag in the main beam of the reader antenna, is subtracted to each tag acquisition thus obtaining the calibrated signal. The signal received from the tag acquisition comprises different kind of contributions. The most significant ones are the *antenna mismatch* (the reflection is due to the mismatch between the cable and the transmitting antenna) and the *multipath* (due to the environment where the tag is situated) while the *tag signature* represents the weakest signal. In addition, if the tag is placed on a box, the latter backscatters a signal which is coming from the same position of the tag and with a much stronger in amplitude. The contributions included into the two acquisitions required for the calibration are summarized as follows:

- **Tag** = Cable/Antenna Mismatch + Tag + Box + Multipath.
- **Background**= Cable/Antenna Mismatch + Multipath.

By subtracting the background ($s_{11}^{background}$) from the measure of the tag (s_{11}^{tag}), the calibrated signal is obtained:

$$s = s_{11}^{tag} - s_{11}^{background} \tag{1}$$

In addition, the movement of the tag allows for several interrogations of the same tag. These multiple acquisitions can be advantageously processed to enhance the received signal and hence the tag signature detection [14]. Obviously, due to the chipless tag movement on the conveyor belt, each of those backscattered signals have accumulated a different phase due to the different path lengths. After the compensation of these phase differences, the signals can be integrated to obtain one single processed signal. Let s_i be the complex frequency response of the tag located at the *i-th* position:

$$s_i = |s_i| \exp\left(j \angle s_i \right) \tag{2}$$

Then, the sum of all the compensated signals s_i^c , is called s^{INT} and it can be written as follows:

$$s^{INT} = \sum_i s_i^c = \sum_i |s_i| \exp\left(j \angle s_i \right) \exp\left(j 2\pi f t_i \right) \tag{3}$$

where t_i is the *i-th* round trip time equal to:

$$t_i = 2d_i / c \tag{4}$$

where d_i is the distance between the reading antenna and the *i-th* position of the tag, f is the working frequency of the chipless tag and c is the speed of light. The number of integrations required to this one-dimension ISAR approach, depends on the -3 dB beamwidth of the antenna. The reading procedure is sketched in Fig. 2.

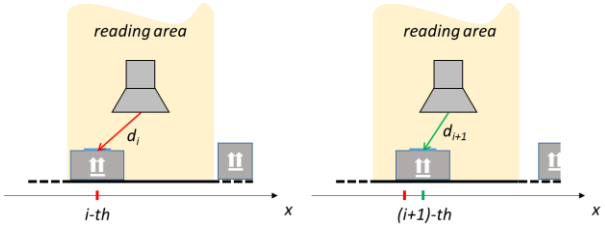

Fig. 2. Reading procedure of a moving chipless tag.

An equivalent view of the moving tag with respect to the fixed transmitting antenna is an array of M elements located in correspondence of the M positions assumed by the moving tag during the reading process. The integration performed on the multiple received signals is equivalent to focusing the beam in the position of the transmitting antenna in the near field region [15].

The basic idea is to compensate the phase difference for each different path, to sum together (constructive interference) the M field contributions at the assigned focal point located in the antenna near field region. Fig. 3 shows the field distribution in the proximity of the reading antenna when a conventional aperture antenna or an array of aperture antennas is employed for reading the tag. In the former case, the field distribution generated by a horn antenna is obtained by discretizing the aperture with 21 closely spaced point sources. In the latter case, the field distribution is fictitious as it is obtained from

the integration of the backscattered signal according to the relation (3).

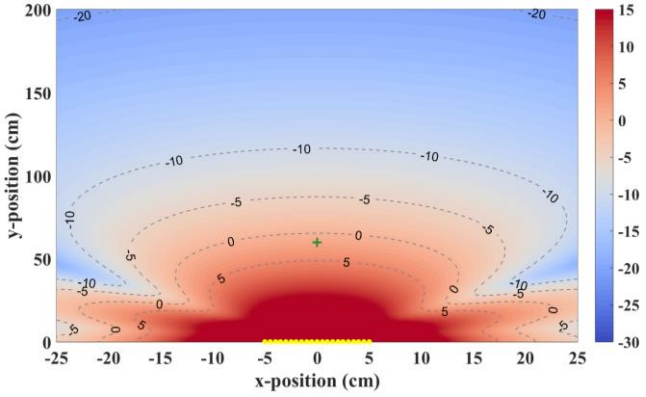

(a)

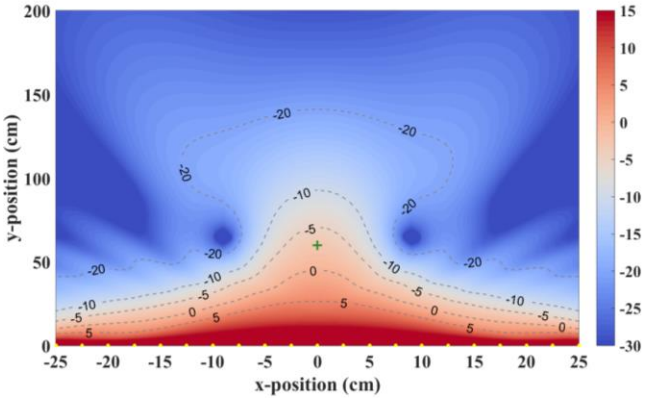

(b)

Fig. 3. (a) Electric field magnitude distribution obtained on a plane containing the tag by using a conventional aperture antenna of 10 cm. The yellow dots on the x-axis represent the locations of the elementary point sources due to the aperture spatial sampling. (b) Electric field generated by a 21 equally-spaced aperture antennas array with the interelement spacing being λ/2. The yellow dots on the x-axis represent the positions of the aperture antennas characterized by a size of 10 cm. The green cross represents the position of the beam focus.

In the case of the ISAR processing, a 21-element array of aperture antennas equally-spaced λ/2 apart, is used. For both Fig. 3(a) and (b), the calculation is performed at 6 GHz (λ_0=5 cm) and the electric field distribution is normalized to the electric field value in the focusing position (*i.e.* the tag position). The parameters used for the two simulations are summarized in Table I.

Table I
PARAMETERS OF THE SYNTHESIZED ANTENNAS WITH NEAR FIELD ELECTRIC DISTRIBUTION PLOTTED IN FIG. 3. SIMULATIONS ARE PERFORMED AT f_0=6 GHZ (λ_0 = 5CM).

	Aperture antenna	**Array of aperture antennas**
$N_{antennas}$	1	21
Antenna size	10 cm	10 cm
$N_{samples}$ per antenna	21	11
Aperture sampling	0.5 cm	1 cm
Total # of point sources	21	231
Antenna spacing	-	2.5 cm

The use of the ISAR processing is equivalent to focus the beam of the reader antenna in the near field region in correspondence of the position of the tag (showed as green cross in Fig. 3). The focusing procedure allows concentrating the electric field on the tags thus drastically reducing the interference by nearby objects.

III. SIGNAL CLUTTER MODEL

As pointed out in the previous section, the use of ISAR processing is equivalent to focus the beam in the position of the reader antenna. Consequently, the effect of multipath and, in general, of the undesired scattered signals coming from other objects is considerably mitigated. In order to theoretically assess the problem, a simplified model comprising two contributions (tag and clutter) described as complex variables in polar form, is adopted. The signal after the background subtraction and after the phase compensation is considered. Therefore, the two contributions represent the useful signal and the undesired signal radiated by the box which is not removable with the background subtraction. The tag signal is represented by a realistic model formed by a shunt connection of an inductance and a capacitance [5]. The inductance represents the impedance of a grounded substrate and the capacitance in series with a resistor represents the Frequency Selective Surface (FSS) equivalent circuit [16]. The frequency response of the tag is characterized by a typical deep absorption peak around the resonance frequency and a rapid phase transition from +180° to -180°. The clutter amplitude is modelled as a normal random process with amplitude |n| and standard deviation equal to the signal amplitude. The phase ϑ_n is modelled as a uniform random process with a variance equal to π. The parameters used to model the amplitude and the phase of the random process are summarized in Table II.

Table II
PARAMETERS USED TO MODEL THE AMPLITUDE AND THE PHASE OF THE NOISE PROCESS.

	Amplitude	**Phase**
Process type	Gaussian	Uniform
Average value	|t|/SNR	0
Variance	(|t|/SNR)^2	$\pi^2/3$

The total received signal, after background calibration, in presence of the clutter (*s*) can be described as the sum of the backscattered signal of the tag (*t*) and the clutter (*n*) as follows:

$$s = |s|\exp(j\vartheta_s) = t + n = |t|\exp(j\vartheta_t) + |n|\exp(j\vartheta_n) \quad (5)$$

The tag information needs to be extracted from the received noisy signal. The decision can be performed by processing either the phase or the amplitude of the signal. With some simple calculations, it is possible to analytically derive both the amplitude and the phase of the disturbed received signal as a function of the signal to noise ratio ($SNR = |t|^2 / |n|^2$):

$$\vartheta_S = \tan^{-1}\left(\frac{\sqrt{SNR}\sin\vartheta_t + \sin\vartheta_n}{\sqrt{SNR}\cos\vartheta_t + \cos\vartheta_n}\right) \approx \vartheta_t \quad if\ SNR >> 1 \quad (6)$$

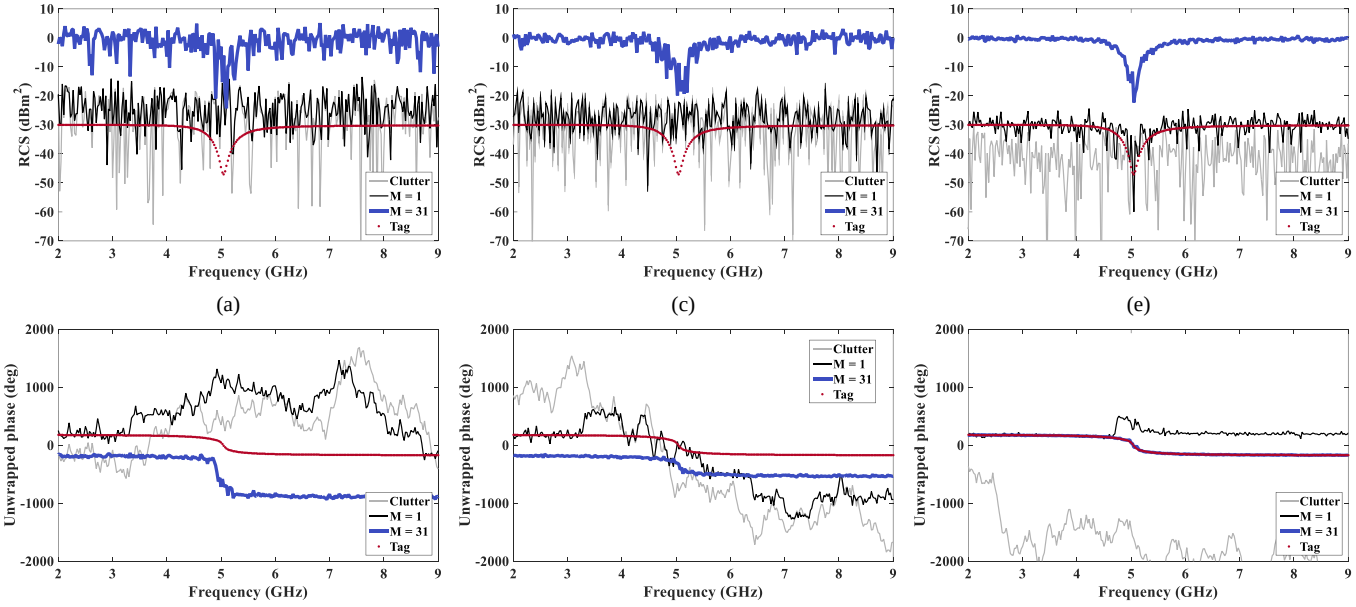

Fig. 4. Amplitude and phase of the total signal (signal and noise) obtained with a single acquisition ($M = 1$) and with $M = 31$ acquisitions according to the simplified model for different values and SNR. (a)-(b) SNR = -5dB, (c) - (d) SNR=0dB, (e) - (f) SNR=10dB. The results are obtained from one realization of the stochastic process of the clutter.

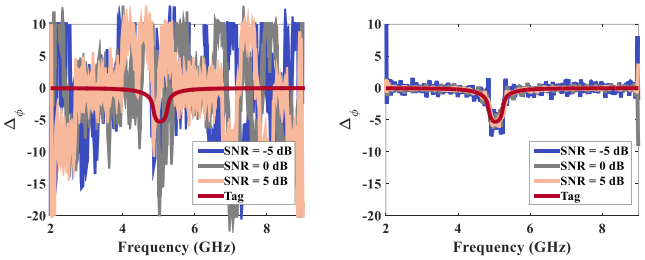

Fig. 5. Phase derivative of the total signal (tag plus clutter) for different levels of SNR. (a) M = 1, (b) M = 31.

$$|s| = \sqrt{SNR + 1 + 2\sqrt{SNR}\left(\cos\vartheta_t \cos\vartheta_n + \sin\vartheta_t \sin\vartheta_n\right)} \approx \sqrt{SNR + 2\sqrt{SNR}\left(\cos\vartheta_t \cos\vartheta_n + \sin\vartheta_t \sin\vartheta_n\right)} \quad if\ SNR >> 1 \tag{7}$$

As evident from relations (6) and (7), when the SNR is reasonably high, e.g. 10 dB, the detected phase converges rapidly to the desired one, that is ϑ_t. On the contrary, the amplitude of the signal $|s|$ converges to $|t|$ more slowly.

For this reason, we can state that it is convenient to exploit the phase of the noisy signal s to perform the detection of the tag instead of the amplitude of the noisy signal. The higher robustness of the phase in the detection of the peaks with respect to the amplitude is confirmed also by experimental results that will be shown in the following sections. The use of ISAR processing allows for collecting multiple measurements of the tag from different interrogation angles and then summing them coherently by removing the phase difference due to the different path lengths. After the removal of the residual phases as in (3), and under the hypothesis that the tag signal be the same independently of the elevation angle of interrogation, the total signal obtained with a number M of interrogations in presence of noise is:

$$s_M^{INT} = \sum_{i=1}^{M} s_i^c = M \cdot s^c + \sum_{i=1}^{M} n_i = M|t|\exp\left(j\vartheta_t\right) + \sum_{i=1}^{M}|n_i|\exp\left(j\vartheta_{n_i}\right) \tag{8}$$

where the superscript c is used to identify the compensated signals. The use of ISAR integration drastically improves the robustness of the detection since the useful part of the received signal is strengthened by the integration of the M measurements. It is worth underling that the integration of M backscattered clutter signals does not affect the SNR level. This is due to the fact that the clutter is not coherently integrated because of its random oscillations in amplitude and phase. Consequently, the integration does not increase the level of the clutter. To demonstrate the viability of the presented method, the proposed analytic model is employed in different scenarios. In particular, the amplitude of the received signal (normalized to 0 dB in the LC model) is scaled to a realistic RCS level. For simplicity, a tag with a single resonance at 5 GHz is considered over the analysed bandwidth ranging from 1 GHz to 10 GHz. In Fig. 4, the RCS of the signal and the phase of the received signal with a single interrogation, M=1, and with M=31 interrogations are represented. Three realizations of the process with three different level of SNR are shown (SNR=–5, SNR=0, SNR=5). The fact that the signal grows up by 30 dB when 31 observations are used depends on the fact that signal is increased by 31 times on average, but RCS is proportional to the square of the scattered field (E^{scatt}) according to:

$$RCS = 20\log_{10}(M \times E^{scatt}) = 10\log_{10}(M^2) + RCS_{dB} \tag{9}$$

A decision algorithm has been also implemented by using the phase of the received signal. In particular, the derivative of the phase of the received signal (Δ_ϕ) is cross-correlated with that of the ideal signal. A realization of Δ_ϕ for the three SNR levels analyzed in previous example is shown in Fig. 5. The figure reports both the phase derivative obtained with a single

measurement ($M = 1$) and with the integration of 31 signals ($M = 31$). All the curves are correlated with the ideal one of the tag (red curve) thus obtaining the correlation coefficient R. A correlation coefficient R higher than 0.8 codifies the bit "1" (presence of the bit). Conversely, R lower than 0.8 codifies the bit "0" (absence of the bit). Based on this decision method, the error probability is then computed for different SNR levels. The BER is finally computed as a function of the SNR by a set of Montecarlo simulations. In particular, 10^6 realizations for both the case of single reading ($M = 1$) and for the ISAR processing with M=31 are used to compute the BER. The estimated BER for this example of a single-bit tag is reported in Fig. 6.

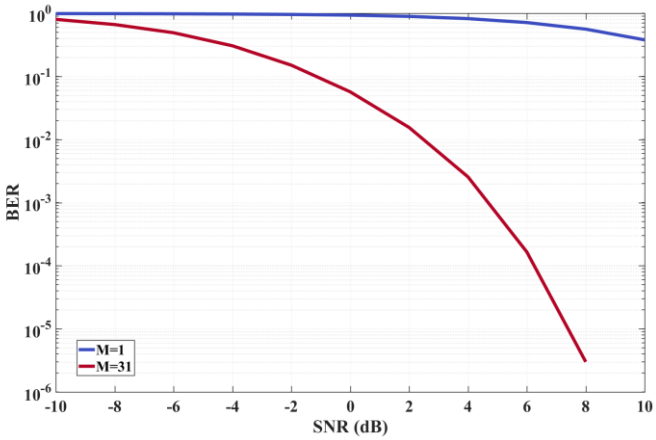

Fig. 6. BER for a single bit tag as a function of the SNR according to the proposed analytical model.

IV. Experimental Verification

The proposed reading procedure for moving chipless RFIDs has been verified by performing an extensive measurement campaign in a non-anechoic environment. A chipless tag whose unit cell is formed by three nested loops has been used for the tests. The chipless RFID tag, which comprises 9 unit cells arranged in a 3 by 3 configuration, is etched on a 1.6 mm thick grounded FR4 substrate. The tag response is characterized by three deep nulls in the reflection coefficient due to absorption [5]. The tag is also characterized by three transitions in the phase profile at the same resonant frequencies in accordance to the model previously employed in Section III. The bit sequence of the tag used as benchmark is 111. The layout of the tag is shown in Fig. 7. The choice of the tag is quite arbitrary and other tag configurations might be employed to this purpose. An important aspect is the presence of the ground plane in the structure of the chipless tag. Since our aim is to test the response of the tag when it is accommodated on highly scattering boxes, the presence of the ground plane is essential [17], [18]. A depolarizing tag could even allow a better isolation of the tag response from disturbing objects, but it requires the use of low loss substrates. The interrogation of the moving tag is carried out by placing the antenna at a distance d_r from the central position of the moving system. The tag is moved on a straight line with M quantized steps of length Δd lower than a half-wavelength. A three-dimensional sketch of the measurement setup is reported in Fig. 8. The number of measurements M stored and used for the integration is estimated based on the 3dB footprint of the reader antenna (θ_{3dB}). According to the measurement setup depicted in Fig. 8, the dimension L of the area illuminated by the main beam of the reader antenna along the direction of the movement of the tag (dimension of the fictitious aperture of the array) is defined as:

$$L = 2d_r \tan\left(\theta_{3dB}/2\right) \tag{10}$$

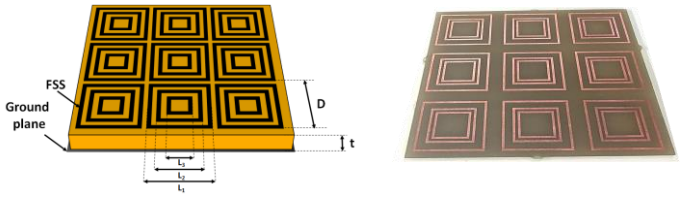

(a) (b)

Fig. 7. (a) Layout of the chipless tag with periodicity D=15 mm employed in the experiments. The total tag size is 4.5 cm by 4.5 cm. The substrate is FR4 with t=1.6 mm. (b) Picture of the fabricated tag.

Once the sampling step Δd is defined, the number of necessary integrations yields:

$$M = \frac{L}{\Delta d} \tag{11}$$

As already remarked, one of the crucial points of this interrogation system is that the antenna is fixed, and this allows the storage of the background response before the tag passes in front of the antenna. Therefore, one of the most important problems of the chipless tags, *i.e.* the background subtraction, is circumvented by using this setup. The background response, named $s_{11}^{background}$, is subtracted from each measurement acquired when the tag is within the main lobe of the antenna according to the relation (1). The presence of the tag, or at least an object, in front of the antenna is detected by observing the signal intensity which substantially increases with respect to the background case. As the presence of a relevant target is detected, the system starts integrating the previously acquired signal and the *M-1* following ones to obtain the overall signal s^{INT}. The time t, required to perform the tag detection, is directly proportional to the tangential velocity v_t of the conveyor belt and can be computed as $t = L/v_t$. Supposing a typical tangential velocity of 0.5 m/s, the time to complete the required trajectory in front of the antenna is roughly one second. It is also possible to calculate the interrogation angle θ_n, the radial velocity of the box v_r for every position $n\,\Delta d$ in the trajectory and thus the Doppler shift f_D as follow:

$$\theta_n = a\tan\left(\frac{L/2 - n\,\Delta d}{d_r}\right) \tag{12}$$

$$v_r = v_t \cos\left(\frac{\pi}{2} - \vartheta_n\right) \tag{13}$$

$$f_D = \frac{2v_r}{\lambda} \tag{14}$$

By using f = 5 GHz and for a tangential velocity equals to 0.5 m/s, the Doppler shift is below 4 Hz and thus negligible.

Another important aspect which is worth mentioning is that the proposed reading method, based on integration of multiple measurements, assumes the tag as a point source with the phase centre located in the middle of the tag. Since the tag is characterized by a finite size, the phase coherence is guaranteed as long as the dimension of the tag does not exceed a certain size. There is a trade-off between the phase coherence of the signal radiated by a single tag and its RCS level. If a single cell is used, the RCS level is so low that the scattered field does not emerge from the noise level at a reasonable distance. On the other hand, the phase coherence of the tag, as in the case of an aperture antenna, is maintained if the tag dimensions are not excessively large. This aspect has been analysed by using the standard array theory approach. The simulations have been performed considering an aperture composed of $N_{elements} \times N_{elements}$ scattering centres spaced by D = 15 mm as in the case of our tag configurations. The phase of the total electric field for a distance d_r equal to 50 cm at 6 GHz for various shift of the tag with respect to the central position of the reader antenna ($X_{positions}$) has been computed. The phase of electric field is then obtained as the summation of scattering centres contributions. The total phase of electric field is plotted in Fig. 9. As is evident, the coherence of the phase is maintained up to a number of elements equal to five.

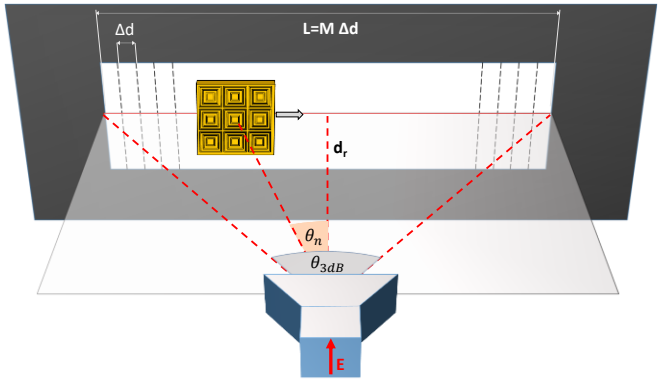

Fig. 8. Three-dimensional sketch of the measurement setup.

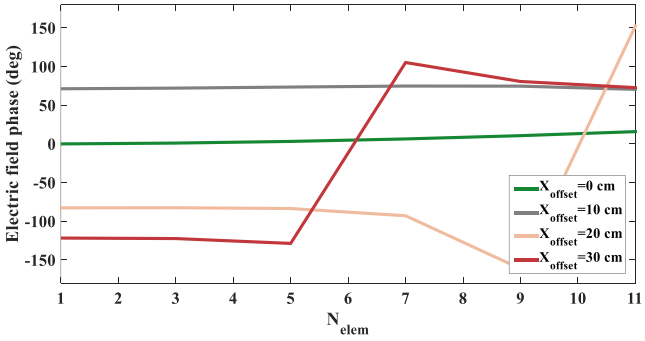

Fig. 9. Phase of the electric field radiated by a N_{elem} linear array with a interelement spacing of D = 15 mm observed on a plane parallel to the array place at a distance d_r=50 cm. The total phase is observed in different points shifted with respect to the boresight direction. The shift is equal to X_{offset}.

Since our tag comprises three elements we can state that the phase coherence is not an issue in this application.

V. Measurement of the Tag in Free Space

The first test of the system has been made by measuring the 3-bit chipless tag in free space at a distance of 130 cm from the interrogating antenna. The tag has been read by using a single measurement with the background subtraction (even if it would not be possible in a realistic scenario) and by using the ISAR integration. The measurements have been performed in a noisy environment. The tag was suspended on a table by using a Styrofoam sample holder and moved along a straight trajectory with discrete steps of 1 cm. The tag has been interrogated through a dual polarized horn antenna (Flann Horn - Model DP240) characterized by a gain of 8 dBi at 2 GHz which increases up to 13.3 dBi at 8 GHz. The vertical polarization is used is this case. This means that the tag is interrogated with TE polarization. The number of processed measurement M was 67. According to the relation (10), the total size of the synthetic aperture L is therefore 67 cm. The distance between the antenna and the tag is determined by looking at the slope of the measured phase. Indeed, the unwrapped phase is characterized by a slope which is proportional to the distance between the phase center of the antenna and the tag. The phase of the 3-bits tag measured at 130 cm from the antenna after the background subtraction is shown in Fig. 10. A linear phase profile ($4\pi\ dr\ f / c$) is used for the fitting of the slope thus estimating the central distance d_r. The optimal distance used to compensate the phases is not exactly the physical distance between the end of the antenna and the tag but it depends on the position of the phase center of the reader antenna which is located inside the antenna. In this case the estimated distance is equal to 145 cm.

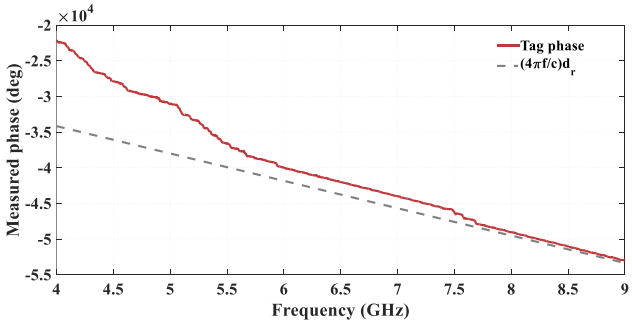

Fig. 10. Measured phase of the tag in the central position after background subtraction.

The derivative of the unwrapped phase (Δ_ϕ) has been used for the detection of the peaks according to the previous discussion in Section III. The received signal obtained with one single measurement in line of sight (LOS) and with the ISAR processing are shown in Fig. 11. It is apparent from the same figure that the ISAR approach gives a much more unambiguous signal with respect to the single measurement setup where the bit sequence is not intelligible. In addition, the single measurement setup relies on the background subtraction performed in absence of the tag that would not be possible in an operative scenario.

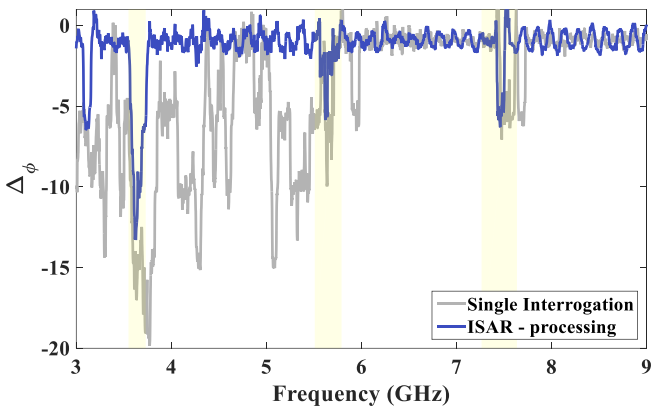

Fig. 11. Comparison between the derivative of the phase obtained with a single measurement in LOS and the derivative of the phase obtained by using the ISAR-based approach. In this case, the distance between the transmitting antenna and the central tag is equal to 130 cm.

On the contrary, the background subtraction is easily applicable for the proposed detection scheme based on the ISAR processing by using the acquisition stored in absence of any obstacle.

VI. Measurement on Highly Scattering Objects

In order to assess the potentialities of the proposed procedure in realistic scenarios, the reading of the tag has been also performed on low and high scattering objects. The objective of these experimental test is to study how the objects inside the box, and thus the level of the clutter, affect the quality of the measurements and hence the tag readability. The tag has been attached to a plastic box filled in a controlled way. The first setup ('box I') includes four tape rolls inside the box on the left and on the right side of the tag but not behind the tag (inset Fig. 12(a)). In the second setup ('box II'), the plastic box is filled with the tape rolls also behind the tag and with a random orientation (inset Fig. 12(b)). In the former case, the distance between the tag and the transmitting antenna is 50 cm. In the latter scenario, the distance between the tag and the transmitting antenna is increased to 80 cm in order to obtain a wider footprint of the main beam of the antenna and thus increasing the number of integrations. The scenario 'box II' at a distance of 50 cm will be also analysed later.

In Fig. 12(a) and (b), the derivative of the phase is reported for the two analysed scenarios. In the first scenario (Fig. 12(a)), a number of integrations equal to 31 is necessary for a correct detection of the bit sequence. In the second scenario Fig. 12 (b), the tag is detected at 80 cm with 45 integrations.
As is evident from Fig. 12(b), a lower number of integrations ($M = 37$) is sufficient to detect two peaks whereas, the classical reading procedure ($M=1$) allows detecting only the third peak. It has to be remarked that, in accordance with the simplified mathematical model discussed in Section IV, the detection of the bit sequence is compromised if the level of the clutter further increases and therefore the SNR decreases to an unacceptable level. Fig. 13 compares the total RCS (tag + clutter), the RCS of the clutter and that of the useful signal for 'box II' scenario. The RCS is computed according to the classical radar equation [18], where the signals obtained after background subtractions represent the ratio between the received and the transmitted power. The detection has been performed with a level of useful signal 5 dB smaller than clutter level ($SNR = -5\ dB$). To further improve the robustness of the detection, it is necessary to reduce the impact of the clutter on the useful signal. This can be achieved employing polarization diversity and depolarizing tags [17]. Depolarizing tags generally exhibit better performance with respect to co-polarized tags since the clutter exhibit the same polarization of the signal generated by the reader antenna thus obtaining an additional level of isolation. It is worth highlighting that the presented reading procedure is also valid for depolarizing chipless tags.

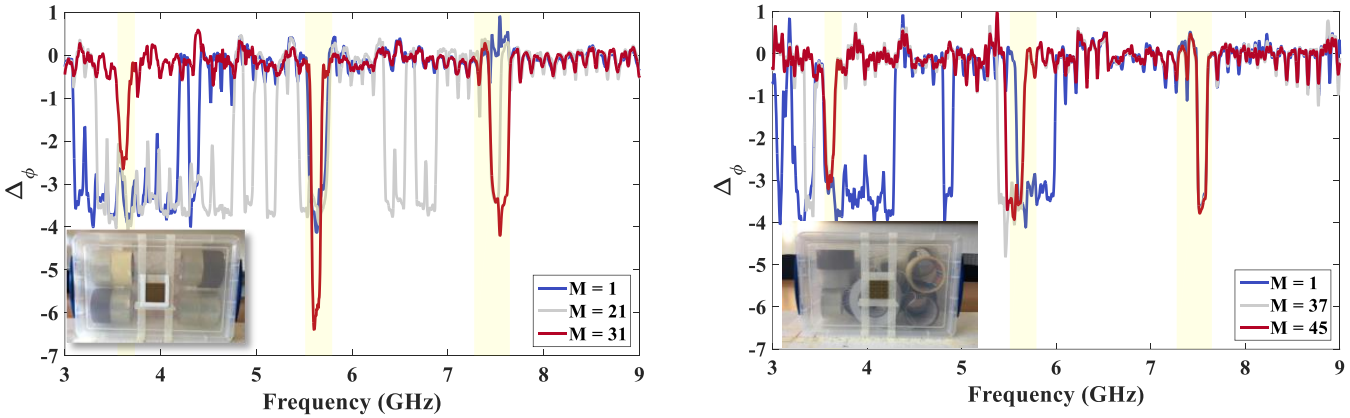

(a) (b)

Fig. 12. Derivative of the phase obtained with a single measurement in LOS (M=1) and the derivative of the phase obtained by using the ISAR-based approach with a different number of integrations. (a) 'box I' at 50 cm, (b) 'box II' at 80 cm.

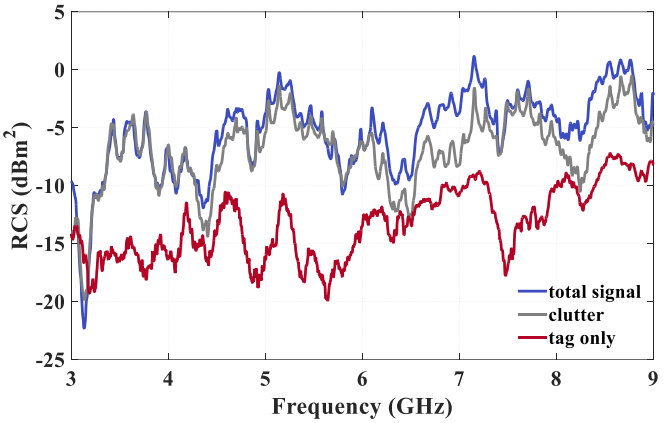

Fig. 13. RCS of the tag compared to the RCS of the clutter and to the total RCS in the case of 'box II'.

VII. Optimal Number of Integrated Signals

A further aspect worthy of discussion is the optimal number of integrations. It has to be pointed out that an indiscriminate increase of the number of integrations is not the optimal solution but it can even deteriorate the quality of the received signal. The first reason is that, if the step interval Δd is not modified, additional acquisitions are performed when the tag is outside the main beam of the antenna. The second reason is that the response of the tag may change with the elevation interrogation angle θ. The simulated reflection amplitude and phase of the tag used in the measurement campaign as a function of the incident angle, for TE polarization, are respectively reported in Fig. 14(a) and (b). As it is evident from Fig. 14(b), the tag employed in the experimental measurements is sufficiently robust with respect to the elevation angle, but the phase response exhibits some deviations when the incident angle is varied over 40 degrees. To overcome this problem, a phase compensation term is introduced in the ISAR formula. This compensation term considers the variation phase response of the tag as a function of θ. This allows to recalibrate the entire system. The phase deviations of the tag with respect to the incident angle can be derived experimentally in a preliminary characterization of the tag analysed in an ideal environment (no clutter). This has been done performing the first acquisition when the tag is moving on the conveyor belt in absence of any objects. The phase responses collected for various incidence angles are used to compute the phase deviation of the tag response with respect to the central position (tag located in front of the transmitting antenna). Assuming s_{TAG}^{i} is the response of the tag at the *i-th* position of the interrogation windows, that is at the angle $\theta_i = tan^{-1}\left((i\Delta_d)/d_r\right)$, and s_{TAG}^{0} is the response of the tag in the central position, the phase compensation term reads:

$$\Delta\phi^i = \angle s_{TAG}^{i} - \angle s_{TAG}^{0} \tag{15}$$

Relation (3) will be therefore modified as follows:

$$S_{compensated}^{INT} = \sum_i \left|S_{11}^i\right| \exp\left(j\angle S_{11}^i\right) \exp\left(j2\pi f t_i\right) \exp\left(-j\Delta\phi^i\right) \tag{16}$$

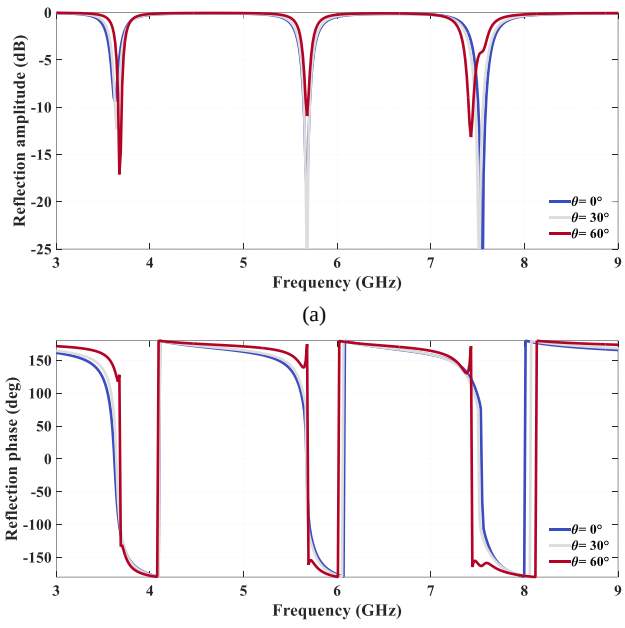

Fig. 14. Simulated reflection coefficient of the 3-bit tag for different incident wave angles.

By applying this procedure, a remarkable improvement in the bit sequence detection has been observed. In order to experimentally prove this point, the measured data with 'box II' at a distance of 50 cm have been considered. Indeed, in this case, it was impossible to detect the second of the three peaks. For this reason, in the example reported in the previous section, the read range was set to 80 cm thus increasing the number of integrations and diminishing the impact of the incident angle variation. By using the tag phase compensation calibration, it is possible to detect all three peaks even at 50 cm. The results of the processing, obtained by using 31 integrations is shown in Fig. 15.

We can conclude that, as a rule of thumb, it would be preferable to stay within an incident angle ranging between ± 45°. This angular sector roughly corresponds to the -3dB beamwidth of a typical reader antenna.

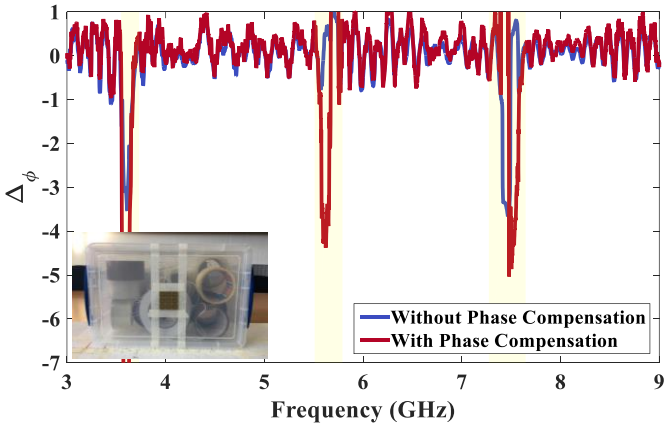

Fig. 15. Derivative of the phase obtained with and without compensation of the tag phase deviation. The scenario is 'box II' at a distance of 50 cm.

VIII. Conclusion

A novel RFID chipless tag detection technique based on the ISAR processing is presented and experimentally verified. The reading technique can be applied for the detection of chipless RFID tags operating in a real scenario. Due to the tag movement, the background subtraction is feasible and thus no additional actions are required to the operator. Moreover, the integration of multiple acquisitions of the same tag in different positions provides a remarkable improvement of the detection accuracy. The detection of a chipless RFID tag with square periodic resonators has been demonstrated in free space for a maximum read range of 130 cm. Subsequently, the tag has been attached on a plastic box which has been filled in a controlled way to study the tag detectability for different levels of clutter. A simplified model has been introduced to clarify how the proposed detection procedure, based on the integration of several acquisitions, provides a drastic improvement of the Bit Error Rate for a certain SNR level. A large set of experimental tests has demonstrated the superiority of the proposed detection scheme with respect to the standard LOS measurement setup, which in turn requires an unfeasible background subtraction.

References

[1] S. Preradovic and N. C. Karmakar, "Chipless RFID: Bar Code of the Future," *IEEE Microw. Mag.*, vol. 11, no. 7, pp. 87–97, Dec. 2010.

[2] S. Tedjini, N. Karmakar, E. Perret, A. Vena, R. Koswatta, and R. E-Azim, "Hold the Chips: Chipless Technology, an Alternative Technique for RFID," *IEEE Microw. Mag.*, vol. 14, no. 5, pp. 56–65, Jul. 2013.

[3] A. Lazaro, A. Ramos, D. Girbau, and R. Villarino, "Chipless UWB RFID Tag Detection Using Continuous Wavelet Transform," *IEEE Antennas Wirel. Propag. Lett.*, vol. 10, pp. 520–523, 2011.

[4] A. T. Blischak and M. Manteghi, "Embedded Singularity Chipless RFID Tags," *IEEE Trans. Antennas Propag.*, vol. 59, no. 11, pp. 3961–3968, Nov. 2011.

[5] F. Costa, S. Genovesi, and A. Monorchio, "A Chipless RFID Based on Multiresonant High-Impedance Surfaces," *IEEE Trans. Microw. Theory Tech.*, vol. 61, no. 1, pp. 146–153, Jan. 2013.

[6] A. Vena, E. Perret, and S. Tedjini, "Chipless RFID Tag Using Hybrid Coding Technique," *IEEE Trans. Microw. Theory Tech.*, vol. 59, no. 12, pp. 3356–3364, Dec. 2011.

[7] D. Girbau, Á. Ramos, A. Lazaro, S. Rima, and R. Villarino, "Passive Wireless Temperature Sensor Based on Time-Coded UWB Chipless RFID Tags," *IEEE Trans. Microw. Theory Tech.*, vol. 60, no. 11, pp. 3623–3632, Nov. 2012.

[8] R. S. Nair, E. Perret, S. Tedjini, and T. Baron, "A Group-Delay-Based Chipless RFID Humidity Tag Sensor Using Silicon Nanowires," *IEEE Antennas Wirel. Propag. Lett.*, vol. 12, pp. 729–732, 2013.

[9] E. M. Amin, M. S. Bhuiyan, N. C. Karmakar, and B. Winther-Jensen, "Development of a Low Cost Printable Chipless RFID Humidity Sensor," *IEEE Sens. J.*, vol. 14, no. 1, pp. 140–149, Jan. 2014.

[10] M. Borgese, F. A. Dicandia, F. Costa, S. Genovesi, and G. Manara, "An Inkjet Printed Chipless RFID Sensor for Wireless Humidity Monitoring," *IEEE Sens. J.*, vol. 17, no. 15, pp. 4699–4707, Aug. 2017.

[11] A. Vena, E. Perret, B. Sorli, and S. Tedjini, "Theoretical study on detection distance for chipless RFID systems according to transmit power regulation standards," in *2015 9th European Conference on Antennas and Propagation (EuCAP)*, 2015, pp. 1–4.

[12] F. Costa, S. Genovesi, and A. Monorchio, "Normalization-Free Chipless RFIDs by Using Dual-Polarized Interrogation," *IEEE Trans. Microw. Theory Tech.*, vol. 64, no. 1, pp. 310–318, Jan. 2016.

[13] A. Ramos, E. Perret, O. Rance, S. Tedjini, A. Lázaro, and D. Girbau, "Temporal Separation Detection for Chipless Depolarizing Frequency-Coded RFID," *IEEE Trans. Microw. Theory Tech.*, vol. 64, no. 7, pp. 2326–2337, Jul. 2016.

[14] A. Buffi, P. Nepa, and F. Lombardini, "A Phase-Based Technique for Localization of UHF-RFID Tags Moving on a Conveyor Belt: Performance Analysis and Test-Case Measurements," *IEEE Sens. J.*, vol. 15, no. 1, pp. 387–396, Gennaio 2015.

[15] A. Buffi, P. Nepa, and G. Manara, "Design Criteria for Near-Field-Focused Planar Arrays," *IEEE Antennas Propag. Mag.*, vol. 54, no. 1, pp. 40–50, Feb. 2012.

[16] F. Costa, A. Monorchio, and G. Manara, "An Overview of Equivalent Circuit Modeling Techniques of Frequency Selective Surfaces and Metasurfaces," *Appl. Comput. Electromagn. Soc. J.*, vol. 29, no. 12, pp. 960–976, 2014.

[17] A. Vena, E. Perret, and S. Tedjni, "A Depolarizing Chipless RFID Tag for Robust Detection and Its FCC Compliant UWB Reading System," *IEEE Trans. Microw. Theory Tech.*, vol. 61, no. 8, pp. 2982–2994, Aug. 2013.

[18] F. Costa, S. Genovesi, and A. Monorchio, "Chipless RFIDs for Metallic Objects by Using Cross Polarization Encoding," *IEEE Trans. Antennas Propag.*, vol. 62, no. 8, pp. 4402–4407, Aug. 2014.

Filippo Costa (S'07-M'11) received the M.Sc. degree in telecommunication engineering and the Ph.D. degree in applied electromagnetism from the University of Pisa, Pisa, Italy, in 2006 and 2010, respectively. In 2009, he was a Visiting Researcher at the Department of Radio Science and Engineering, Helsinki University of Technology, TKK (now Aalto University), Finland.

He is currently an Assistant Professor at the University of Pisa. His research interests include metamaterials, metasurfaces, antennas and Radio Frequency Identification (RFID). He serves as an Associate Editor of the IEEE SENSORS LETTERS. In 2015 and 2016, he was appointed as outstanding reviewer of IEEE TRANSACTIONS ON ANTENNAS AND PROPAGATION. He was recipient of the Young Scientist Award of the URSI International Symposium on Electromagnetic Theory, URSI General Assembly and URSI AT-RASC in 2013, 2014 and 2015, respectively.

Michele Borgese (S'17) received B.E. and M.E. degrees in telecommunications engineering from the University of Pisa, Italy, in 2010 and 2013, respectively. In 2017, he received the PhD degree in Ingegneria dell'Informazione from the University of Pisa where he is currently a Post-Doctoral Researcher at the Microwave and Radiation Laboratory. Currently, he is involved in the design of multiband reflactarrays and chipless RFID sensors.

Antonio Gentile received Bachelor and M.Sc. degree in Telecommunications Engineering from the university of Pisa, Pisa, Italy, in 2013 and 2016, respectively. From August 2016, he is Research Assistant at the Microwave and Radiation Laboratory, Information Department, University of Pisa. From February 2017 to December 2017, he was a Visiting Researcher at University Rovira i Virgili, Tarragona, Spain, working on chipless RFID sensors.

Luca Buoncristiani received Bachelor and M.Sc. degree in telecommunications engineering from the University of Pisa, Italy, in 2013 and 2016, respectively. In 2016, he was Research Assistant at the Microwave and Radiation Laboratory, Dipartimento dell'informazione, University of Pisa. During

the period 2016-2017 he was a Visiting Researcher at University Rovira I Virgili, working on chipless RFID sensors. Currently he is with U-blox and he is involved in design and testing of cellular modules.

Simone Genovesi (S'99-M'07) received the Laurea degree in telecommunication engineering and the Ph.D. degree in information engineering from the University of Pisa, Pisa, Italy, in 2003 and 2007, respectively. He is currently an Assistant Professor at the Microwave and Radiation Laboratory, University of Pisa. Current research topics focus on metamaterials, radio frequency identification (RFID) systems, optimization algorithms and reconfigurable antennas. He was the recipient of a grant from the Massachusetts Institute of Technology in the framework of the MIT International Science and Technology Initiatives (MISTI).

Francesco Alessio Dicandia (S'16) received the bachelor's and master's degrees in telecommunications engineering from the University of Pisa, Pisa, Italy, in 2012 and 2014, respectively, where he is currently pursuing the Ph.D. degree. His current research interests include reconfigurable antennas, multiple-input and multiple-output antennas, non-Foster matching network, characteristic modes analysis, and chipless RFID sensors.

Davide Bianchi (S'13-M'17) was born in Livorno, Tuscany, IT, in 1983. He received the B.S. and M.S. degrees in Telecommunication engineering from The University of Pisa, IT, in 2006 and 2008, respectively. After being the recipient of a grant issued by the italian Ministry of Education and Science (MIUR), in 2013 he receiveid the Ph.D. degree in remote sensing engineering at the Pisa University Department of Information Engineering. Since 2009 Mr. Bianchi has been affiliated with the National InterUniversity Consortium for Telecommunications (CNIT) which presented him with a research grant in the field of antenna theory and design for HF-Skywave radar applications. In 2010 he was presented with a 2009-2010 FSE (European Social Fund) Graduate Student Award and he was a visiting student in the Pennsylvania State University (Penn State) at the Computational Electromagnetics and Antennas Research Lab (CEARL), University Park. Since 2012 he has been affiliated with the National Laboratory Radar and Surveillance (RaSS) and he is currently a Postdoctoral Research Fellow for the Microwave and Radiation Lab (MRL) at the University of Pisa. His main research topics include computational electromagnetics and evolutionary strategies with applications to ultrawideband and phased array design as well as conformal antenna optimization and miniaturization. Other interests include parallel and high performance computer programming.

Agostino Monorchio (S'89–M'96–SM'04–F'12), Professor at the Department of Information Engineering of the University of Pisa, is active in a number of areas related to electromagnetics, including computational numerical techniques, microwave metamaterials, radio propagation for wireless systems, the design and miniaturization of antennas and electromagnetic compatibility, microwaves biomedical applications.

Giuliano Manara received the Laurea (Doctor) degree in electronics engineering (summa cum laude) from the University of Florence, Italy, in 1979. Currently, he is a Professor of the University of Pisa, Italy. From 2000 to 2010 and since 2013, he has been serving as the President of the Bachelor and the Master Programs in Telecommunications Engineering at the same University. Since 2010, he has been serving as the President of the Bachelor Program in Telecommunications Engineering at the Italian Navy Accademy in Livorno, Italy. Since 1980, he has been collaborating with the Department of Electrical Engineering of the Ohio State University, Columbus, Ohio, USA, where, in the summer and fall of 1987, he was involved in research at the ElectroScience Laboratory.

His research interests have centered mainly on the asymptotic solution of radiation and scattering problems. He has also been engaged in research on numerical, analytical and hybrid techniques, frequency selective surfaces (FSS) and electromagnetic compatibility. More recently, his research has also been focused on antenna design and on Radio Frequency Identification (RFID).

Prof. Manara was elected an IEEE (Institute of Electrical and Electronic Engineers) Fellow in 2004 for "contributions to the uniform geometrical theory of diffraction and its applications.". He served as the International Chair of URSI Commission B for the triennium 2011-2014. Prof. Manara has served as the General Chair of the International Symposium on Electromagnetic Theory (EMTS 2013), held in Hiroshima, Japan, May 20-24, 2013.

Prof. Manara is the President of CUBIT (Consortium UBIquitous Technologies) S.C.A.R.L., a consortium created by the Dipartimento di Ingegneria dell'Informazione of the University of Pisa, Polo Navacchio S.p.A. (Navacchio, Cascina) and some highly innovative Italian companies, with the aim of defining a new knowledge transfer model from university to industry.